Effects of electron–irradiation darkening and its posterior bleaching by light in novel Cr–Mg–YAS fiber

Article *in* Laser Physics Letters · December 2016

DOI: 10.1088/1612-2011/13/12/125103

CITATIONS
0

READS
31

9 authors, including:

A. V. Kir'yanov
Centro de Investigaciones en Optica
246 PUBLICATIONS **1,570** CITATIONS
SEE PROFILE

Yuri O Barmenkov
Centro de Investigaciones en Optica
153 PUBLICATIONS **1,188** CITATIONS
SEE PROFILE

Anirban Dhar
Central Glass and Ceramics Research Institute
98 PUBLICATIONS **620** CITATIONS
SEE PROFILE

Mukul Paul
Central Glass and Ceramics Research Institute
173 PUBLICATIONS **726** CITATIONS
SEE PROFILE

Effects of electron-irradiation darkening and its posterior bleaching by light in novel Cr–Mg–YAS fiber

2016 Laser Phys. Lett. 13 125103

(http://iopscience.iop.org/1612-202X/13/12/125103)

IOP Publishing | Astro Ltd
Laser Physics Letters
Laser Phys. Lett. **13** (2016) 125103 (9pp)
doi:10.1088/1612-2011/13/12/125103

Letter

Effects of electron-irradiation darkening and its posterior bleaching by light in novel Cr–Mg–YAS fiber

A V Kir'yanov[1,3], D Dutta[2], Y O Barmenkov[1], S Das[2], A Dhar[2], M C Paul[2], S I Didenko[3], S A Legotin[3] and K I Tapero[3,4]

[1] Centro de Investigaciones en Optica, Loma del Bosque 115, Col. Lomas del Campestre, Leon 37150, Guanajuato, Mexico
[2] Fiber Optics and Photonics Division, CSIR- Central Glass & Ceramic Research Institute, 196 Raja S.C. Mullick Road, Kolkata-700032, India
[3] National University of Science and Technology (NUST) 'MISIS', Leninsky Avenue 4, Moscow 119049, Russia
[4] Research Institute of Scientific Instruments, Lytkarino, Industrial Zone 'Turaevo' 8, Moscow Region 140080, Russia

E-mail: kiryanov@cio.mx and paulmukul@hotmail.com

Received 2 June 2016, revised 23 October 2016
Accepted for publication 23 October 2016
Published 7 November 2016

Abstract

Two remarkable effects for the recently invented chromium–magnesium (Cr–Mg) co-doped yttria-alumino-silicate fiber are reported: (i) strong and spectrally peculiar darkening under the action of energetic (6 MeV) β-electrons with dosage up to 1.0×10^{15} cm^{-2} and (ii) posterior optical bleaching of the darkening loss at exposure to low-power (of a mW-range) 633 nm light. Both phenomena are revealed to be conspecific to co-doping the fiber with Mg and to the presence of versatile valence forms of Cr ions. The reported results seem to be impactful for exploiting fiber of such type for dosimetry and in space technology.

Keywords: chromium-doped optical fiber, fibers characterization, optical bleaching, electron irradiation

(Some figures may appear in colour only in the online journal)

1. Introduction

In this letter, we report the effects of high-energy β-electron irradiation (βI), resulting in spectrally peculiar induced absorption, or 'darkening', and its posterior low-power optical bleaching (OB) for the recently fabricated yttria-alumino-silicate (YAS) fiber co-doped with chromium (Cr) and magnesium (Mg) [1–3] (further—Cr–Mg–YAS).

As known to the authors, no study was carried out to-date about the effect of βI upon optical properties of Cr-doped fibers, although such researches, albeit very few, were reported on the susceptibility of bulk Cr-doped glasses to βI [4–6]. Meanwhile, the knowledge of βI related changes in attenuation and fluorescence spectra (at optical excitation), occurring in a doped optical fiber, deserves a big deal of attention given that it helps, on one hand, in uncovering general essences of the phenomena involved (see e.g. [7–12]) and, on the other hand, it may serve for clarifying particular sides of βI, useful for applications such as dosimetry and space technologies. For instance, dosimetry systems are invaluable for sensing high-radiation fields in proximity to nuclear reactors and hazardous places, due to versatile physical effects in radiation-sensitive silica fibers (see e.g. [12, 13]).

When a doped glassy medium, e.g. silica fiber doped with rare-earths or transitional/post-transitional metals, is

subjected to any kind of ionizing radiation, such as γ-quanta, neutrons, β-electrons, it is 'darkened'. Darkening means rise, as the result of ionization, of extinction in characteristic bands of dopants and other inherent defects of the fiber's core-glass. As a rule, darkening is more expressed in doped materials as compared to un-doped ones because dopants can themselves be sources of secondary carriers, appearing in the form of free electrons and holes or excitons, which—after annihilating or trapping on imperfections of core-glass (e.g. on dopants)—can be responsible for a diversity of radiation-induced defects and color centers being born. Accordingly, transformations arise in fluorescence spectra, characteristic to dopants and color centers generated as the result of ionization. Namely these phenomena permit the use of a doped optical fiber for effective sensing dosage of ionizing radiations, e.g. βI. As shown below, Cr–Mg–YAS fiber presents a relevant choice to reach the target, given that βI-darkening is much more notable in this fiber as compared, say, to Cr–YAS (Mg-free) and standard SMF-28 ones (taken in this study as reference).

Furthermore, we report a pronounceable effect of posterior OB of β-darkened Cr–Mg–YAS fiber, in terms of absorption and fluorescence spectra' transformations, at its treatment under low-power VIS (633 nm, a mW-range) illumination. In contrast, we revealed negligible OB at exposing darkened Cr–Mg–YAS fiber to NIR light @1070 nm, in similar conditions. The choice of these two wavelengths for OB the darkened Cr–Mg–YAS fiber was defined by their spectral matching in VIS-to-NIR with the bands of induced absorption (IA), arising as a result of βI, and with the 'natural' ones, characteristic to Cr ions in multiple valence states. Furthermore, whereas a part of IA in VIS, fading at OB @633 nm, was measured by hundreds of dB m^{-1} in Cr–Mg–YAS fiber, no OB effect was detected by us in βI-darkened Cr–YAS and SMF-28 reference fibers. (Note that OB has been recently reported for βI-darkened cerium-doped silica fiber [7] but its appearance was merely different to what happens with Cr–Mg–YAS fiber.)

Needless to say, an opportunity to 'medicate' βI-darkened Cr–Mg–YAS fiber, *viz.* to restore—at least partially—its former state by means of OB, deserves attention as a measure, invaluable for practical applications. Indeed, for a fiber-based sensor placed in the harmful environment of a nuclear plant for detecting ionizing radiation, where access is hardly permitted or denied, a prerequisite is assessing multiple cycles of sensing (i.e. measuring irradiation-induced darkening or the fading of dopants' fluorescence), enabled via intermixing with periods of 'renewing', or 'refreshing', the sensor's head. Exploiting the OB phenomenon to refresh βI-darkened Cr–Mg–YAS fiber to be used as a sensor of ionizing radiations of multiple usage seems to be indispensable.

Apart from reporting and discussing in detail the spectral transformations in absorptive and fluorescent properties, experienced by the fibers under study after βI and OB, we also report their 'counterparts', fingerprinted in cross-sectional images, at white-light (WL) microscopy. These data provide a piece of further information, useful for visualization of both phenomena.

Cr–Mg–YAS fibers, fabricated entirely through the modified chemical vapor deposition/solution-doping (MCVD/SD) technique, were recently shown to be capable—when pumped at wavelengths falling into the Cr-related absorption bands—of pronounceable fluorescence in VIS-to-NIR (much more intensive in NIR as compared to fibers free from co-doping with Mg). This feature was revealed to stem from Cr^{4+} ions in such Cr–Mg–YAS fibers, formed due to charge compensation [2, 3]. Details of fabrication of Cr–Mg–YAS fibers are provided in [1]. Notice that at making Cr–Mg–YAS preforms we underwent a MCVD/SD route where soaking solutions (in water and alcohol) were $AlCl_3.6H_2O$, $Y(NO_3)_3.6H_2O$, $CrCl_3.6H_2O$, and $MgCl_2.6H_2O$ and that final acrylate-coated Cr–Mg–YAS fibers, quite uniform through length, were drawn to ≈12/125 μm core/cladding diameters with numerical apertures ≈0.2…0.25. As stemmed from the HRTEM/SAED and Raman-scattering analyses, these Cr–Mg–YAS fibers demonstrate entirely amorphous structure without any phase-separation of core-glass [3].

Of the current study scope was a sample of such-type Cr–Mg–YAS fiber (fabricated using the same routine as the fibers spectroscopically analyzed in detail in [3]) and its comparison, in terms of susceptibility to βI and OB, with samples of Cr–YAS (Mg-free) fiber (drawn by a similar way) and commercial SMF-28 fiber.

2. Experimental arrangement

For βI, a controllable linear accelerator, emitting β-electrons with a narrow-band energy spectrum (~6 MeV) in a short-pulse (~5 μs) mode [7, 9, 14], was employed. Below, βI-dosage is exemplified by 1.3×10^{11} (dose '1'), 1.3×10^{12} (dose '2'), 2.9×10^{13} (dose '3'), 1.0×10^{14} (dose '4'), and 1.0×10^{15} (dose '5') cm^{-2}. Samples of Cr–Mg–YAS, Cr–YAS, and SMF-28 fibers, 1 to 2 m in length, were placed into the accelerator's chamber for various time intervals, providing 'snapshots' of growing irradiation dosage. The irradiated fibers were left for two weeks for relaxation prior to making the main-course measurements—in order to avoid the role of short components in decay of (IA), established after βI. The spectral measurements proceeded during a limited time (*viz.*, during the following two weeks) for diminishing the effect of spontaneous IA-recovery. Note that ionization, i.e. production at βI of secondary holes and electrons (free or in the form of excitons), seems to be the main cause of the spectral transformations to be reported (high-energy primary β-electrons are virtually non-dissipating at propagating through a fiber sample). However, γ-quanta born at inelastic scattering of β-electrons cannot be disregarded as another factor contributing to the overall ionization of the fiber's core-glass.

Optical transmission spectra of fiber samples were measured employing the cutback method, with a white-light (WL) source and optical spectrum analyzer (OSA). Such spectra were recorded before and after each βI-dose or time of exposure to 633/1070 nm lights, launched from laser diodes (LDs).

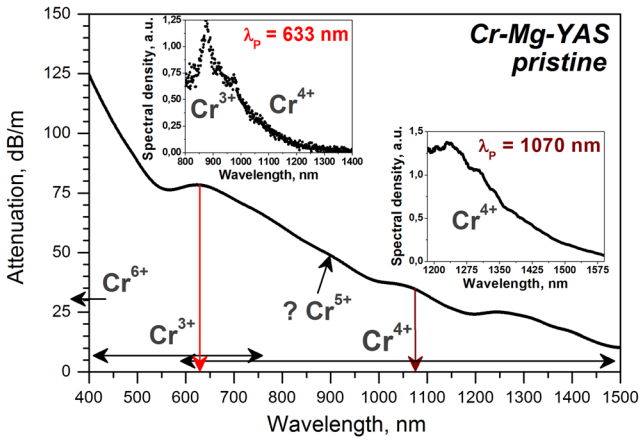

Figure 1. (Main-frame) Attenuation spectrum of the Cr–Mg–YAS fiber in pristine state, with the contributions of Cr ions in different valence states ($Cr^{3+}/Cr^{4+}/Cr^{5+}/Cr^{6+}$) being specified by horizontal arrows. (Insets) Characteristic (to Cr^{3+} and Cr^{4+} ions) fluorescence spectra of the fiber, obtained at excitations of 633 (left) and 1070 (right) nm.

The attenuation spectra presented below were obtained after recalculating the measured transmission into loss.

Fluorescence of the Cr–Mg–YAS fiber (in pristine, β-darkened, and OB states) was under study, too. (As the reference Cr–YAS (Mg-free) fiber is much less active in fluorescence [3] whilst un-doped SMF-28 fiber is vastly emission-inactive, we omitted such measurements with these two fibers.) The fluorescence spectra were obtained, using the OSA, at excitation by the same LDs in two detecting schemes: 'forward' (@633 nm) and 'backward' (@1070 nm). In the first case, the spectra were registered by capturing fluorescence on fiber output (the rest of pump light, though significant, did not affect much the essences of Cr related fluorescence, mostly presented in NIR). In the second one, we employed a kind of backward counting (see figure 2 in [3]), permitting LD's spontaneous emission (SE) component to be filtered out, tailing up to 1300 nm and thus obscuring visualization of NIR fluorescence (Cr^{4+} ions).

The transmission dynamics of β-darkened Cr–Mg–YAS fiber at OB was monitored in frontal detecting geometry. In this case, light @633/1070 nm, delivered to a fiber sample, was measured on the fiber output by a power-meter, allowing detection of the changes in its transmission *in situ*.

The fibers' cross-sectional images were obtained using an optical microscope at WL illumination; we handled in this case 0.5 cm pieces of 90°-cleaved fibers (being in pristine, β-darkened, or OB state).

3. Results and discussion

3.1. Pristine fibers

The attenuation spectrum of the pristine (as-received) Cr–Mg–YAS fiber is shown in figure 1.

As seen from the figure, the fiber demonstrates intensive absorption bands in UV, VIS and NIR. First, note that Mg ions are 'inactive' in the sense of extinction within UV/VIS/NIR spectral ranges; so, the bands appearing in figure 1 entirely belong to Cr ions being in versatile valent forms. Based on the available data on Cr-doped silicate glasses and glass-ceramics (core-glass of the Cr–Mg–YAS fiber is a kind of Cr-doped silica glass), see e.g. [3] and references therein and [4–6], these bands are attributed as follows. The bands in VIS (@450…750 nm) are assigned to (*d*–*d*) transitions $^4A_2 \rightarrow {}^4T_1$ and $^4A_2 \rightarrow {}^4T_2$ of Cr^{3+} ions in octahedral coordination, while the band in UV (not shown) to the charge-transfer transition of Cr^{6+} ions, as well in octahedral coordination. In turn, the bands at wavelengths longer than 650 nm in VIS and in NIR attribute the presence of Cr^{4+} ions in tetrahedral coordination, with the correspondent transitions being $^3A_2 \rightarrow {}^3T_1$, $^3A_2 \rightarrow {}^3T_2$ (@650…1150 nm) and $^1E \rightarrow {}^3T_2$ (>1200 nm) [1, 3]. (A contribution in absorption within an 850…950 nm interval, see elevation in this spectral range, can stem from the Cr^{5+} ions' presence but is questionable.) This is schematized in figure 1 by the horizontal arrows, specifying the spectral intervals, characteristic to absorption of Cr ions being in $Cr^{3+}/Cr^{4+}/Cr^{5+}/Cr^{6+}$ valence states. As seen from the figure, Cr^{6+}/Cr^{3+} and Cr^{3+}/Cr^{4+} related absorption bands are superimposed at wavelengths <500 nm and @600…750 nm, correspondingly, which hardens explicit decomposition of the fiber's overall absorption spectrum into separate, well-defined, bands. Furthermore, the vertical arrows in figure 1 designate the spectral positions of excitation (@633/1070 nm), chosen to characterize the fiber's fluorescent properties. The point to mention here is that excitation at 633 nm mainly falls into the absorption band of Cr^{3+} ions, whereas that at 1070 nm matches the absorption band, mostly belonging to Cr^{4+} ions. The two insets in figure 1 exemplify the characteristic fluorescence spectra of Cr–Mg–YAS fiber, obtained at 633 and 1070 nm excitations. It is relevant to propose that in the first case VIS-to-NIR fluorescence is produced by both Cr^{3+}/Cr^{4+} ions whereas in the second case NIR fluorescence adheres to solely Cr^{4+} ions.

The fluorescence spectra of the pristine Cr–Mg–YAS fiber, obtained at different pump powers at 633 and 1070 nm, are presented in figures 2(a) and (b), respectively. The spectra were measured handling forward (633 nm, (a)) and backward (1070 nm, (b)) geometries, correspondingly. The difference in samples' lengths taken in these two circumstances was defined by the difference in extinctions at 633 and 1070 nm; refer to figure 1. It is seen that both sets of the spectra are offset on tails of the pumps' SE components, but, despite this, their parts in VIS/NIR are easily assigned as belonging to Cr^{3+}/Cr^{4+} ions.

3.2. β-darkened fibers

In figures 3(a) and (b), we demonstrate the attenuation spectra of Cr–Mg–YAS and SMF-28 fibers, both passed through βI-doses '1' to '5'; note that hereafter colors of the curves represent different βI-doses. We also provide in the figures the attenuation spectra of these fibers being in pristine state, by black curves. The result of βI (exemplified by dose '5') is furthermore compared, for Cr–Mg–YAS and Cr–YAS (Mg-free)

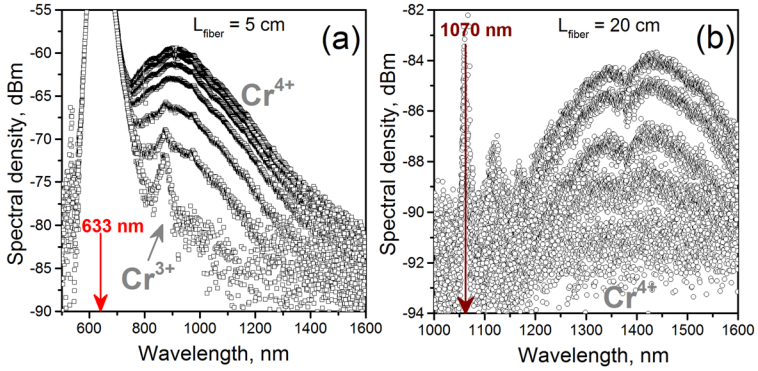

Figure 2. Fluorescence spectra of pristine Cr–Mg–YAS fiber, obtained at different levels of excitation at (a) 633 nm (up to 27 mW) and (b) 1070 nm (up to 170 mW).

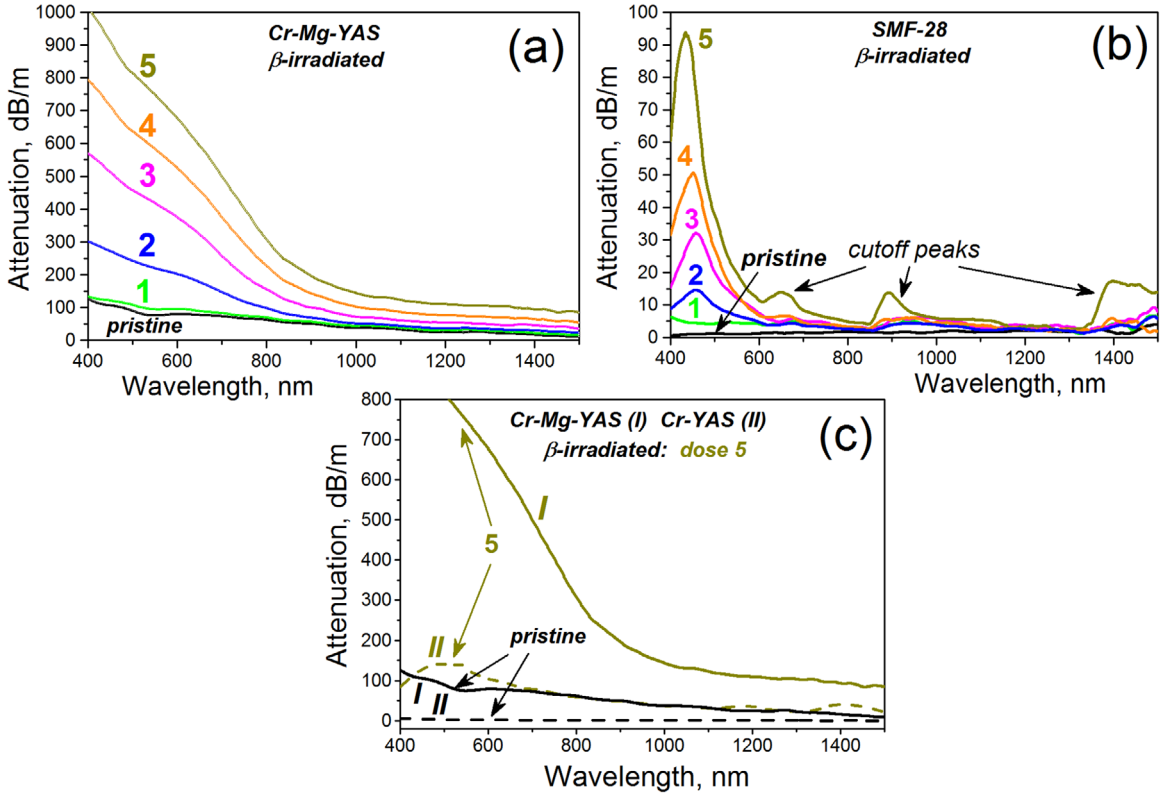

Figure 3. Attenuation spectra of (a) Cr–Mg–YAS and (b) SMF-28 fibers, subjected to βI with doses '1' to '5' (colored curves); for comparison, attenuation spectra of pristine fibers are also shown (black curves). (c) Attenuation spectra of Cr–Mg–YAS (curves I) and Cr–YAS (curves II) fibers, obtained in pristine state (dashed curves) and after βI-dose '5' (solid curves).

fibers, in figure 3(c). We handled in these experiments pieces of fibers measured by <1 to $\approx$10 cm (Cr–Mg–YAS) and $\approx$5 to $\approx$50 cm (Cr–YAS and SMF-28), given that the degree of darkening in the former fiber was, overall, much bigger (by an order of value, reaching few hundreds dB m^{-1} in VIS) than in the latter ones (limited by a hundred dB m^{-1}).

The first thing seen from (a) versus (b) comparison is that IA-growth in Cr–Mg–YAS and SMF-28 fibers notably differs in magnitude: being limited (at maximal dose '5') by $\approx$100 dB m^{-1} in SMF-28 (at $\approx$450 nm), it reaches $\approx$1000 dB m^{-1} ($<$500 nm) in Cr–Mg–YAS. The other thing is that IA in these two types of fiber strongly differs spectrally. IA in SMF-28 fiber spectrally covers UV–VIS (400…600 nm) and can be assigned to increasing with dose of the number of non-bridging oxygen-hole centers (NBOHC) of two types and other defects—such as Si- and Al-related defect centers. In contrast, IA-growth in Cr–Mg–YAS fiber spans a much broader (UV–VIS–NIR) spectral range (whilst IA-elevating within 400…600 nm interval, assigned above for un-doped SMF-28 fiber, can be captured as well). Given that core-glass of both types of fibers is a kind of alumino-silicate glass, this difference should be related to the presence in Cr–Mg–YAS fiber of Cr/Mg co-dopants, absent in the SMF-28 one. Accordingly, two hypotheses can be proposed to explain the difference:

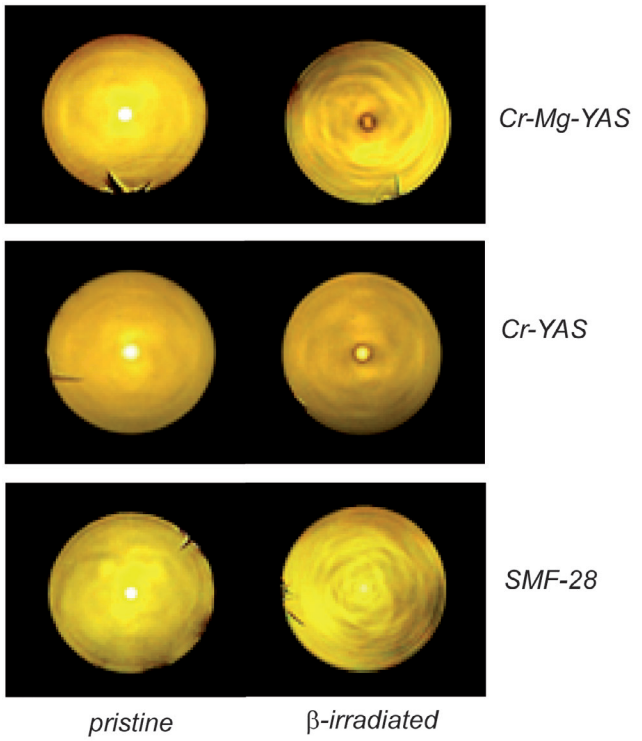

Figure 4. Cross-sectional images of Cr–Mg–YAS (top), Cr–YAS (middle) and SMF-28 (bottom) fibers, photographed in pristine (left column) and βI-darkened (dose '5') (right column) states.

(i) βI in Cr–Mg–YAS fiber leads to valence transformation within an ensemble of valence states of Cr ions (Cr^{2+}/Cr^{3+}/Cr^{4+}/Cr^{5+}/Cr^{6+}), with a guessed result being an increase of contents of Cr^{2+}, Cr^{5+} and Cr^{4+} ions and, correspondingly, a decrease of contents of the Cr^{6+} and Cr^{3+} ones (according to [4–6], Cr ions in glass are mainly subjected, at βI, to reactions of the reduction type, while their presence hardens generating of other defects of glass);

(ii) Mg ions (helping in the formation of Cr^{4+} ions in Cr–Mg–YAS fiber), are—as 'heavy' co-dopants—a powerful source of additional carriers (excitons or free electrons and holes) under bombarding by β-electrons, thus, facilitating formation of defect centers (of both types—inherent to silica core-glass and associated to the presence in core of Cr ions) and, in the meantime, strengthening the re-charging processes among Cr ions, mentioned in *(i)*.

A justification of (ii) can be the data presented in figure 3(c), where we straightforwardly compare the attenuation spectra of Cr–Mg–YAS (solid curves) and Cr–YAS (dashed curves) fibers, obtained after βI-dose '5' (we also provide in this figure the attenuation spectra of these two fibers in pristine state; see black curves). It is seen that the spectrum of Cr–YAS fiber, suffered βI, is quite similar to the one of SMF-28 fiber, irradiated at the same dose '5' (spectrum 5 in figure 3(b)). However, it strongly differs from the one of Cr–Mg–YAS fiber, suffered dose '5' (spectrum 5 in figure 3(a)). This uncovers a notable role of Mg ions in strengthening of βI-darkening in Cr–Mg–YAS fiber.

In figure 4, we present microscopic images of cross-sectional areas of all fibers, Cr–Mg–YAS (top), Cr–YAS (middle), and SMF-28 (bottom), being in pristine (the left column) and βI-darkened (at dose '5') (the right column) states.

It is seen that the core region of Cr–Mg–YAS fiber (especially, its adjacent to cladding area) strongly suffers from βI-darkening—more pronounceably than it happens with reference Cr–YAG and SMF-28 fibers. Moreover, in Cr–Mg–YAS fiber, darkening takes slightly elliptical shape, most probably, indicating stronger stresses arising after βI. A trend of darkening degree to dominate on the core-cladding interface can be explained by the already referred [1, 2] property of partially losing a considerable amount of Cr ions at the collapsing/drawing stages at fabricating preform/fiber of this type. As seen from figure 4 (compare top and middle versus bottom photos), this pattern of darkening arises in both Cr-doped fibers—Cr–Mg–YAS (in a higher degree) and Cr–YAS (in a lesser degree) but not—in the un-doped SMF-28 one.

Figure 5 helps in understanding what happens with the emissive properties of Cr–Mg–YAS fiber after βI. We demonstrate in figure 5(a) only the NIR fluorescence spectra at 1070 nm excitation (in backward geometry), obtained for pristine and βI-darkened (at dose '4') Cr–Mg–YAS fiber, for exemplifying the effect, while its dose dependence is presented in figure 5(b).

It is seen from figure 5(a) that NIR fluorescence (adherent to Cr^{4+} ions) strongly fades as the result of βI (by $\approx$5 dB), which seems to be useful for sensing. Besides, as it can be concluded from figure 5(b), NIR fluorescence, shown by emission power @1425 nm where it is maximal, obeys an almost exponential law of fading versus βI-dose, which gets saturated at doses exceeding 10^{14} cm^{-2}.

Note that we do not consider here how affected is the fluorescent ability of the fiber after βI at 633 nm excitation since, as shown below (see figure 9), this kind of excitation results in fast (minutes) OB of IA, which makes it vastly impossible to reliable capture fluorescence spectra using OSA. Meanwhile, although the OB-effect is detectable as well at 1070 nm excitation—while it is much less effective and slower (see figure 10)—it did not prevent collecting the data shown in figure 5.

3.3. OB-fibers

It is known that darkening of glass, arising under the action of ionizing radiations, can fade, or 'bleach', by light: see e.g. [7, 15–17]. Below, we present the data, evidencing a spectacular OB-effect in VIS in βI-darkened Cr–Mg–YAS fiber, when treating it under the action of low-power 633 nm light. However, negligible or no OB was revealed for the reference βI-darkened Cr–YAS (Mg-free) and SMF-28 fibers.

In OB experiments, light at wavelengths 633 or 1070 nm (delivered from the same LDs, employed for excitation of Cr-related fluorescence) was directly coupled into βI-darkened Cr–Mg–YAS samples. We handled short pieces of

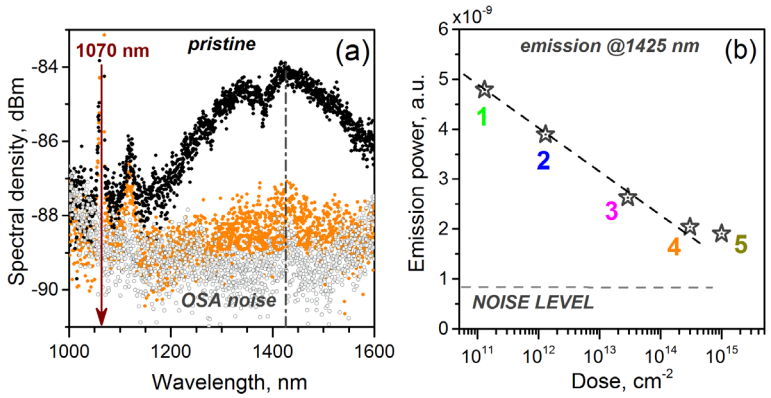

Figure 5. (a) NIR fluorescence spectra of Cr–Mg–YAS fiber in pristine (black dots) and βI-darkened (dose '4') (orange dots) states, at 1070 nm (170 mW) excitation; OSA noise is shown by gray dots. (b) Dependence of emission power @1425 nm (wavelength at which maximal fluorescence signal in NIR is observed) versus βI dosage.

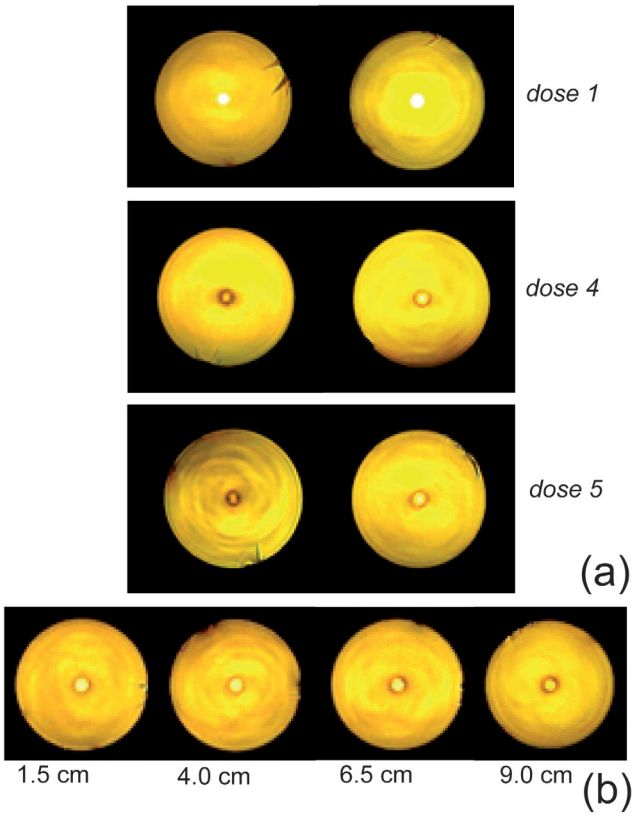

Figure 6. (a) Cross-sectional images of Cr–Mg–YAS fiber, obtained after primary βI (left column) and posterior OB @633 nm (27 mW, ≈3.5 h.) (right column) treatments, with βI-doses being '1' (top), '4' (middle) and '5' (bottom). (b) Cross-sectional images of 11 cm Cr–Mg–YAS fiber, βI-darkened with dose '5' and subsequently OB @633 nm (27 mW) during ≈11 h, obtained at distances 1.5, 4.0, 6.5 and 9.0 cm (left to right), as counted from the point of launching bleaching light @633 nm.

the fiber in this case (1…5 cm, depending on the degree of darkening in VIS). The basic results obtained demonstrate the changes in the fiber's darkening patterns (figure 6) and in attenuation (figure 7) and fluorescence (figure 8), after OB. Then, the results revealing OB dynamics in time domain—in terms of changes in transmission @633/1070 nm of darkened Cr–Mg–YAS fiber—are reported (figure 9). In this case, we varied the length of β-darkened samples and power of bleaching light—to attest the effect in detail.

Figure 6(a) demonstrates the microscopic WL-images of Cr–Mg–YAS fibers (5.5…6 cm in length), first passed through different doses ('1'—top, '4'—middle, and '5'—bottom) of βI, see the left-hand photos, and then (posterior to the treatment) subjected to OB at 633 nm (at maximal launched power, 27 mW) during ≈3.5 h, see the right-hand photos. In the second case, the images were obtained from fiber cuts, spaced by ≈1 cm from the point where bleaching light was launched. It is seen that, overall, the degree of darkening of the fiber's core-area becomes considerably diminished, even for the highest βI-doses. Furthermore, figure 6(b) exemplifies WL-images of a longer (11 cm) Cr–Mg–YAS fiber sample, primarily darkened at βI-dose '5' and then passed through OB during ≈11 h. These photos were obtained for the fiber segments, distant from the point of launching 633 nm light by 1.5, 4.0, 6.5 and 9 cm. It is seen that the bleaching degree of the core-area is comparable in each 'snapshot', thus revealing the opportunity to almost completely recover the initial state of fiber of this type.

Figure 7 provides complementary information to the optical microscopy data (figure 6), that is, the spectral 'signature' of the OB effect. In the main frame of figure 7, at the bottom, we plot the spectra of attenuation difference, *viz.* portion of βI-loss, experiencing bleaching under the action of 633 nm (27 mW) light. For comparison, analogous spectra, measured after OB by 1070 nm light of the same power, are given as an example in the inset. We also provide in figure 7, at the top, the attenuation spectrum of pristine Cr–Mg–YAS fiber, for making an easier comparison of the spectral character of the loss fading at OB, termed in the main-frame as the attenuation difference, with the characteristic absorption bands of Cr ions (assigned in figure 1).

It is seen from figure 7 that OB is much more effective in Cr–Mg–YAS fiber (in terms of bleached βI-loss) at 633 nm than at 1070 nm treatment, though spectrally the βI-loss part, experienced bleaching, looks similar, at both OB kinds. The other thing to emphasize is that the spectral character of attenuation difference (in other words, the bleached part of βI-loss) severely differs from the one detected in pristine Cr–Mg–YAS

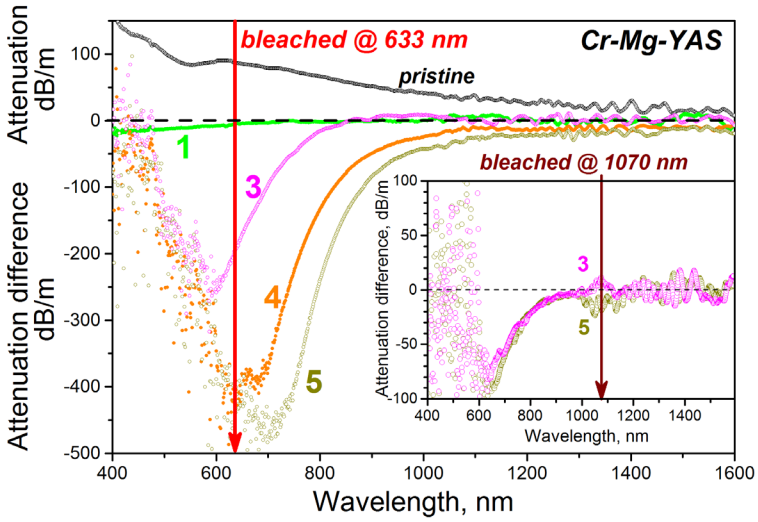

Figure 7. (Bottom) Spectra of attenuation difference between the βI-darkened and OB-bleached states of Cr–Mg–YAS fiber, in the latter case subjected to OB @633 nm (main-frame) and @1070 nm (inset) of the same (27 mW) power. The spectra of different colors correspond to different βI-doses (all spectra were collected at handling the same lengths, 6 cm, of βI-darkened Cr–Mg–YAS fiber samples). (Top) Attenuation spectrum of pristine Cr–Mg–YAS fiber. The arrows schematize the spectral positions of the LDs lines (633 and 1070 nm).

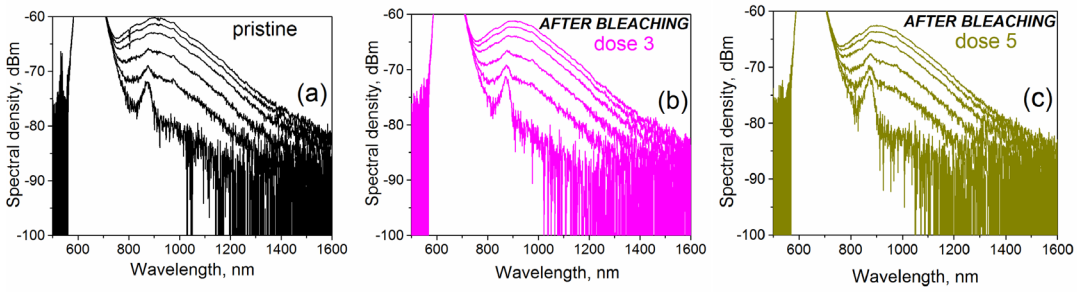

Figure 8. Fluorescence spectra of (a) pristine and (b) and (c) βI-darkened (doses '3' and '5', respectively) and subsequently OB-bleached @633 nm (after 4 h, 27 mW) Cr–Mg–YAS fiber, at varying excitation levels @633 nm.

fiber (where, according to the attributions made in figure 1, valence forms Cr^{6+}, Cr^{3+} and Cr^{4+} dominate in overall extinction): this part spans a broad (500…1200 nm) region, where, in accord with the current viewpoint on the matter [4–6, 17], the absorption bands of Cr^{5+} and Cr^{2+} (along with Cr^{3+}/Cr^{4+}) ions are located. It is noteworthy that the contents of namely the latter ions were argued (in section 3.2) to grow as the result of βI, through a kind of re-charging phenomena, in Cr–Mg–YAS fiber. Hence, it is quite probable that reverse, or backward, processes can go at OB, resulting in the partial recovery of the initial (prior to βI) state of the fiber. However, a more detailed study is required in future to confirm or to reject the above hypotheses.

In figure 8, we demonstrate the NIR fluorescence spectra of Cr–Mg–YAS fiber pumped at 633 nm, being in pristine state (a) and after passing through the cycles of βI (with high doses) followed by OB at 633 nm (with maximal available power and for long exposure time), (b) and (c). These data can serve as a justification that OB leads to recovery, at least partial, of the initial—before subjecting to βI—emissive potential of the fiber. As seen from comparison of (a) versus (b) and (c), only an insignificant portion of fluorescence power has been lost, whereas the character of fluorescence saturation at increasing pump power at 633 nm remained almost unchanged, after completing 'medicating' the fiber by means of OB. This fact seems to be in favor for a renewable Cr–Mg–YAS fiber-based sensor of β-electrons to be invented.

Aiming for a complete description of the OB effect, briefly consider the transmission dynamics of β-darkened Cr–Mg–YAS fiber when applying such a treatment, monitored in time; see figures 9 and 10.

In these figures, we present a set of dependences (versus time) that output power at 633 (figure 9) and 1070 nm (figure 10), escaping β-darkened Cr–Mg–YAS fiber samples, takes. Note that light at these wavelengths was delivered from the LDs into fiber under study directly, through a splice, and its transmitted power was measured by a power-meter. Since the OB phenomenon is spectacular in Cr–Mg–YAS fiber at 633 nm lightening (remind that no OB was detected in the reference Cr–YAS and SMF-28 fibers at either wavelength), we provide its characterization in more detail for this case.

The most featuring results are shown in panels (a)–(c) of figure 9 (note the log–log scaling used):

(i) OB dynamics is exemplified for different βI-doses ('1', '3', '4' and '5') while keeping the same fiber length (5.5…6 cm) and launched power (maximum, 27 mW);

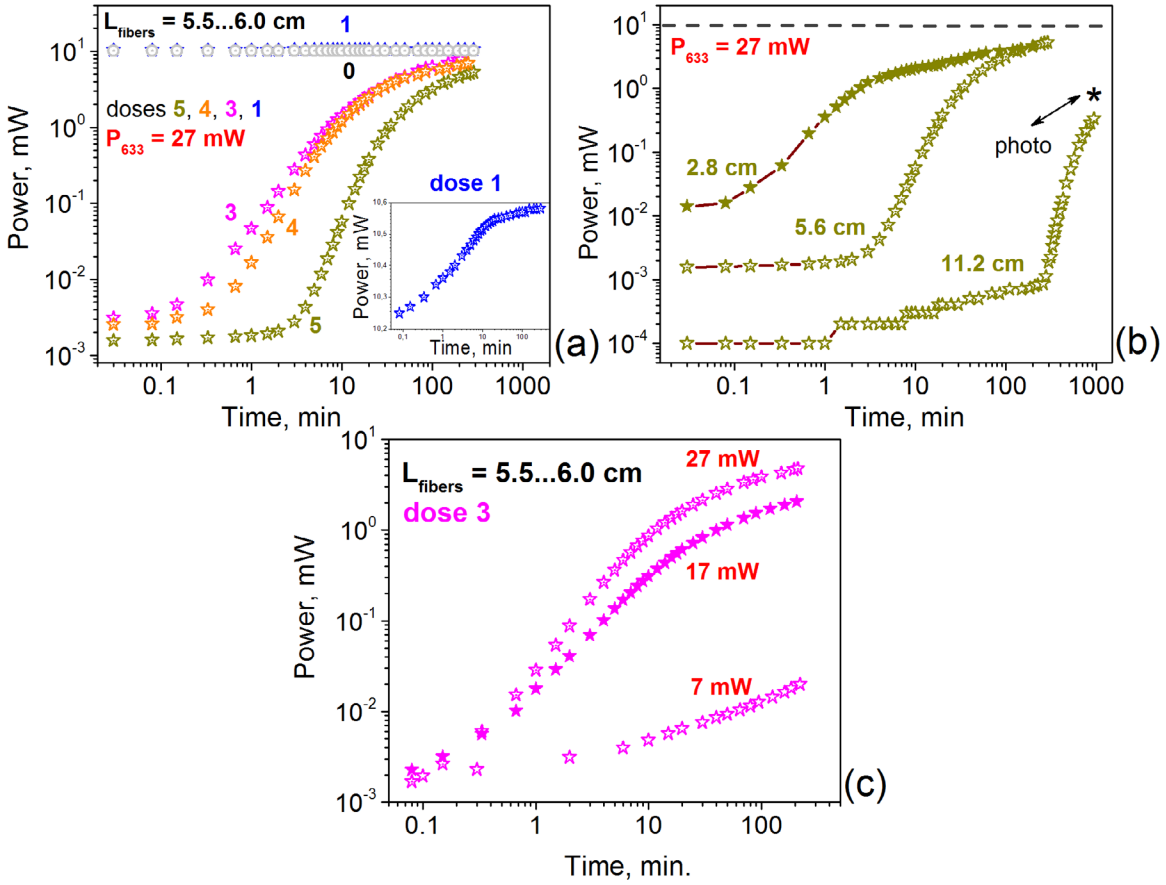

Figure 9. Dynamics of OB, in terms of transmitted power versus time of 633 nm light launched to Cr–Mg–YAS fiber samples, primarily βI-darkened: (a) at different doses—'1', '3', '4' and '5' (symbol '0' labels a pristine sample) but with the same length of samples treated (5.5…6 cm) and fixed power of launched light (27 mW); (b) at different lengths of samples treated (2.8, 5.6 and 11.2 cm) but with fixed power of launched light (27 mW) and the same dose ('5'), applied at βI-darkening; (c) at different OB powers at 633 nm (7, 17 and 27 mW) but with fixed length of samples (5.5…6 cm) and the same dose ('3') of βI. Note that the asterisk in (b) corresponds to terminating OB, for the 11 cm sample, after which the fiber was inspected using WL microscopy (see the results plotted in figure 6(b)).

furthermore, it is compared with the case labelled '0' when pristine fiber of this type was under test: figure 9(a);

(ii) OB dynamics is compared, for the fibers having different lengths (up to ≈11 cm) while darkened at the highest βI-dose ('5'), subjected to maximal launched power @633 nm: figure 9(b);

(iii) OB dynamics is sampled for the fibers, βI-darkened at the same dose ('3'), all having similar lengths (5.5…6 cm), under the action of 633 nm light of various powers (7, 17 and 27 mW): figure 9(c).

For comparison, we also provide, in figure 10, the dependences obtained for Cr–Mg–YAS fiber, at its illuminating at the other available wavelength (1070 nm) but at the same launched power (27 mW), that is, in the conditions analogous to the ones of figure 9(a); notice the linear scaling used in this case.

From the data demonstrated in figures 9 and 10, a few laws that the OB phenomenon obeys can be revealed.

First (compare figures 9(a) and 10), whereas OB at 633 nm is prominent, resulting in notable recovery of the initial (prior

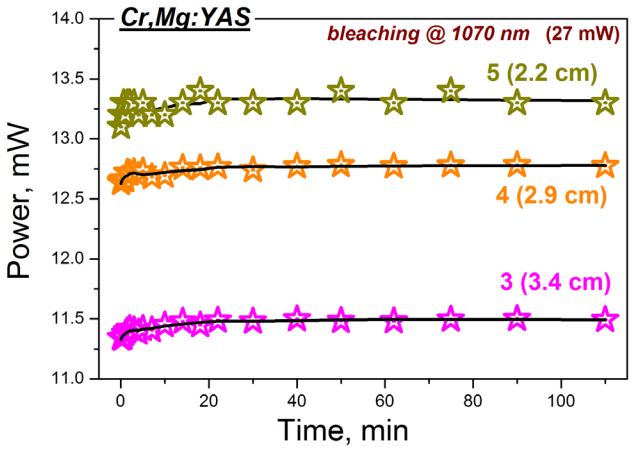

Figure 10. Dynamics of OB, in terms of transmitted power versus time of 1070 nm light launched to Cr–Mg–YAS fiber samples, primarily βI-darkened at different doses ('3', '4' and '5') but the same power of launched light (27 mW); sample lengths treated were 3.4, 2.9 and 2.2 cm, respectively, giving comparable attenuations of fiber prior to OB.

to βI) state-of-the-art of Cr–Mg–YAS fiber in the sense of transmission at this wavelength (which increases by a few orders of value), OB at 1070 nm is negligible (rise of transmission in this case does not exceed 1…2%). Second, OB by VIS light, at 633 nm, is governed by a few simple rules: (i) the higher βI-dose the fiber suffers, the longer time is necessitated for βI-loss to bleach (figure 9(a)); (ii) the longer βI-darkened fiber is exposed to OB, the slower is recovery time of transmission (moreover, this dependence is strongly nonlinear versus fiber length) (figure 9(b)); (iii) the higher power at which OB is proceeding, the faster is the process (this dependence seems to be as well nonlinear but this requires further clarifications) (figure 9(c)).

Before we conclude, notice that, in contrast to the βI-effect itself, which can be explained from the viewpoint of the physics involved (argued in section 3.2), the OB-effect in βI-darkened Cr–Mg–YAS fiber needs a relevant explanation because it is hardly explainable at the moment. We can only propose here that a mechanism behind it can be a kind of optically induced process (involving excitons' generation and trapping/de-trapping of carriers on Cr ions being in polyvalent valences in the core-glass, resulted in re-charging [4–7, 11, 12, 17, 18]). As well, the thermal mechanism cannot be disregarded as potentially relevant to explain OB, especially, at high IA established after βI (when notable optical power is transformed to heat). However, a separate study is required in the future to verify these hypotheses.

4. Conclusions

The data reported in this letter reveal, for the first time to the best of our knowledge, the phenomenology of the βI and OB (at wavelengths 633/1070 nm) effects concerning the basic properties of Cr–Mg–YAS fibers. These phenomena are defined, overall, by a high susceptibility of Cr ions being in polyvalent states and the notable role of Cr/Mg co-doping—given that their appearance in fiber of this type is considerably different as compared with either Cr–YAS (Mg-free) or un-doped (SMF-28) fibers, chosen as reference in this study. Thus, fiber of Cr–Mg–YAS or similar type, where both βI and OB effects are well-expressed and can be gathered, seem to be a good choice for making an all-fiber sensor, possessing of internal re-cycling property, for dosimetry and space technology.

Acknowledgments

A Kir'yanov acknowledges financial support from the Ministry of Education and Science of the Russian Federation through the Increase Competitiveness Program of NUST MISiS through Grant K3-2015–056. The Indian team acknowledges support from the Department of Science and Technology—Nano-Mission, Government of India. One of the Indian coauthors, D Dutta, thanks the DST, Govt. of India, for providing Senior Research Fellowship.

References

[1] Dutta D, Dhar A, Kir'yanov A V, Das S, Bysakh S and Paul M C 2015 Fabrication and characterization of chromium-doped nanophase separated yttria-alumina-silica glass-based optical fibers *Phys. Status Solidi* a **212** 1836

[2] Dutta D, Dhar A, Das S, Bysakh S, Kir'yanov A and Paul M C 2015 Chromium doped nano-phase separated yttria-alumina-silica glass based optical fiber preform: fabrication and characterization *Proc. SPIE* **9654** 96541J

[3] Kir'yanov A V, Dutta D, Barmenkov Y O, Das S, Dhar A, Koltashev V V, Plotnichenko V G and Paul M C 2016 Basic and peculiar properties of chromium-magnesium co-doped YAS-based optical fibers *IEEE J. Quantum Electron.* **52** 6800112

[4] Ollier N, Champagnon B, Boizot B, Guyot Y, Panczer G and Padlyak B 2003 Influence of external β-irradiation in oxide glasses *J. Non-Cryst. Solids* **323** 200

[5] Boizot B, Olivier F Y, Petite G and Ghaleb D 2008 Blocking of alkaline migration under ionizing irradiation in Cr-doped oxide glasses *Nucl. Instrum. Methods. Phys. Res.* B **266** 2966

[6] Malchukova E, Boizot B, Olivier F Y, Petite G and Ghaleb D 2009 Irradiation effects in oxide glasses doped with transition and rare-earth elements *Eur. Phys. J. Appl. Phys.* **45** 107101

[7] Kir'yanov A V, Ghosh S, Paul M C, Barmenkov Y O, Aboites V and Kozlova N S 2014 Ce-doped and Ce/Au-codoped alumino-phospho-silicate fibers: spectral attenuation trends at high-energy electron irradiation and posterior low-power optical bleaching *Opt. Mater. Express* **4** 434

[8] Malchukova E, Boizot B, Petite G and Ghaleb D 2007 Optical properties and valence state of Sm ions in aluminoborosilicate glass under β-irradiation *J. Non-Cryst. Solids* **353** 2397

[9] Kir'yanov A V, Dvoyrin V V, Mashinsky V M, Il'ichev N N, Kozlova N S and Dianov E M 2011 Influence of electron irradiation on optical properties of bismuth doped silica fibers *Opt. Express* **19** 6599

[10] Lombard P, Ollier N and Boizot B 2011 EPR study of Ti^{3+} ions formed under beta irradiation in silicate glasses *J. Non-Cryst. Solids* **357** 1685

[11] Malchukova E and Boizot B 2010 Reduction of Eu^{3+} to Eu^{2+} in aluminoborosilicate glasses under ionizing radiation *Mater. Res. Bull.* **45** 1299

[12] Berthold J W III 1994 Overview of prototype fiber optic sensors for future application in nuclear environments *Proc. SPIE* **2425** 74

[13] Houston A L, Justus B L, Falkenstein P L, Miller R W, Ning H and Altemus R 2001 Remote optical fiber dosimetry *Nucl. Instrum. Methods Phys. Res.* B **184** 55

[14] Ivleva L I, Kozlova N S and Kir'yanov A V 2010 Influence of electron irradiation on optical properties of scheelite crystals *Laser Phys.* **20** 635

[15] Peng M, Zhao Q, Qiu J and Wondraczek L 2009 Generation of emission centers for broadband NIR luminescence in bismuthate glass by femtosecond laser irradiation *J. Am. Ceram. Soc.* **92** 542

[16] Ou Y, Baccaro S, Zhang Y, Yang Y and Chen G 2009 Effect of gamma-ray irradiation on the optical properties of PbO–B_2O_3–SiO_2 and Bi_2O_3–B_2O_3–SiO_2 glasses *J. Am. Ceram. Soc.* **93** 338

[17] Monke D 2015 Photo-ionization of 3d-ions in fluoride-phosphate glasses *Int. J. Appl. Glass Sci.* **6** 249

[18] Kaczmarek S M, Chen W and Boulon G 2006 Recharging processes of Cr ions in Mg_2SiO_4 and $Y_3Al_5O_{12}$ crystals under influence of annealing and γ-irradiation *Cryst. Res. Technol.* **41** 41